




Transcriptome analysis of wild-type and *afsS* deletion mutant strains identifies synergistic transcriptional regulator of *afsS* for a high antibiotic-producing strain of *Streptomyces coelicolor* A3(2)

Min Woo Kim¹ · Bo-Rahm Lee² · SungYong You³ · Eun-Jung Kim² · Ji-Nu Kim² · Eunjung Song² · Yung-Hun Yang⁴ · Daehee Hwang⁵ · Byung-Gee Kim^{1,2} 

Received: 1 November 2017 / Revised: 1 February 2018 / Accepted: 4 February 2018 / Published online: 17 February 2018

© Springer-Verlag GmbH Germany, part of Springer Nature 2018

Abstract

Most secondary metabolism in Actinobacteria is controlled by multi-layered, gene-regulatory networks. These regulatory mechanisms are not easily identified due to their complexity. As a result, when a strong transcriptional regulator (TR) governs activation of biosynthetic pathways of target antibiotics such as actinorhodin (ACT), additional enhancement of the biosynthesis is difficult in combination with other TRs. To find out any “synergistic transcriptional regulators (sTRs)” that show an additive effect on the major, often strong, transcriptional regulator (mTR), here, we performed a clustering analysis using the transcriptome datasets of an mTR deletion mutant and wild-type strain. In the case of ACT biosynthesis in *Streptomyces coelicolor*, PhoU (SCO4228) and RsfA (SCO4677) were selected through the clustering analysis, using AfsS (SCO4425) as a model mTR, and experimentally validated their roles as sTRs. Furthermore, through analysis of synergistic effects, we were able to suggest a novel regulation mechanism and formulate a strategy to maximize the synergistic effect. In the case of the double TR mutant strain (Δ *rsfA* pIBR25::*afsS*), it was confirmed that the increase of cell mass was the major cause of the synergistic effect. Therefore, the strategy to increase the cell mass of double mutant was further attempted by optimizing the expression of efflux pump, which resulted in 2-fold increase in the cell mass and 24-fold increase in the production of ACT. This result is the highest ACT yield from *S. coelicolor* ever reported.

Keywords Combination of transcriptional regulators · Clustering analysis · Time-series transcriptome · Actinorhodin · *Streptomyces coelicolor*

Min Woo Kim and Bo-Rahm Lee contributed equally to this work.

Electronic supplementary material The online version of this article (<https://doi.org/10.1007/s00253-018-8838-3>) contains supplementary material, which is available to authorized users.

✉ Byung-Gee Kim
byungkim@snu.ac.kr

¹ Interdisciplinary Program for Biochemical Engineering, Seoul National University, Seoul, South Korea

² School of Chemical and Biological Engineering, Institute of Molecular Biology and Genetics, and Bioengineering Institute, Seoul National University, Seoul, South Korea

³ Division of Cancer Biology and Therapeutics, Departments of Surgery & Biomedical Sciences, Cedars-Sinai Medical Center, Los Angeles, CA 90048, USA

⁴ Department of Microbial Engineering, College of Engineering, Konkuk University, Seoul, South Korea

⁵ Department of New Biology and Center for Plant Aging Research, Institute for Basic Science, DGIST, Daegu, Republic of Korea

Introduction

Microorganisms are an important source for producing various secondary metabolites useful for the human such as antibiotics, herbicides, and antifungal and anticancer agents (Baltz 2008). Due to the high industrial value of these secondary metabolites, many studies were undertaken to understand and exploit the secondary metabolism. Secondary metabolites are not essential for cell growth and development but help the producing cells to adapt and survive under the surrounding environment. Biosynthetic pathways in the secondary metabolism are tightly regulated by environmental changes such as nutrient depletion, growth phase, and signal transduction to optimize the metabolism in response to various environmental changes (Patra et al. 2013). Therefore, in order to improve production yield of such secondary metabolites, it is important to understand the detailed and phase-dependent regulations of the cell according to environmental changes.

Transcriptional regulator (TR) is a DNA-binding protein that regulates gene expression in response to environmental changes by binding to a specific DNA sequence as an activator or repressor (Patra et al. 2013). Since secondary metabolism is often regulated by a number of TRs (Ohnishi et al. 2005), the metabolism can be more effectively reconstructed to increase the production of target molecules through simultaneous regulation of expression of several TRs. However, due to the complexity of the TR network, it is very difficult to obtain synergistic effect of TRs when a strong TR primarily dominates biosynthetic activation of target secondary metabolism.

In general, there are two groups of TRs: a pathway-specific TR that controls a specific metabolic pathway gene cluster and a global TR that exerts pleiotropic effects on multiple gene clusters by either having the same consensus binding sequence or following the same signal transduction pathway. Secondary metabolism is under the control of both types of TRs in multi-layered, complex, regulatory networks (Lv et al. 2014). Owing to the nature of these multi-layered regulation networks, the interactions of the TRs in hidden layers are not easily predictable, unless the interaction is quite significant. A number of approaches to understanding these networks are common, such as chromatin-immunoprecipitation coupled with massive parallel sequencing (ChIP-Seq) for genome-wide profiling of DNA-protein interactions (Valouev et al. 2008) and DNA-affinity capture assay (DACA) to identify the TRs binding to the promoter region of specific genes (Park et al. 2009). Despite these methods, elucidation of all the networks of TRs in a given organism is difficult, labor-intensive, and time-consuming tasks.

In this work, we performed a clustering analysis using DNA chip data to find a combination of TRs that can exert synergistic effects in complex TR networks without the need to understand TR network or prior knowledge. Clustering analysis enables us to separate and classify the genes with the same expression patterns (Eisen et al. 1998). This method assumes that the TR genes classified into the same cluster are likely to be under the same or similar control networks (Eisen et al. 1998). Thus, clustering analysis can be used to select candidate TRs that have synergistic effects among them. Here, *Streptomyces coelicolor* and actinorhodin (ACT) were selected as a model strain and target molecule, respectively, since the most abundant transcriptomic DNA chip data from public database are available for its physiological and metabolism studies. There are two assumptions to find a synergistic combination of TRs; first, important genes related to secondary metabolism such as major TR (mTR) show highly dynamic transcriptome profile changes during all growth phases and second, the changes in the expression profile of the specific mTR do not affect the expression of synergistic TR (sTR), as sTRs are likely to belong to an upper layer than the specific mTR, or can play an independent role in the same layer. Based

on these assumptions, clustering analysis was performed using time-series transcriptome data of *afsS* deletion mutant ($\Delta afsS$) and parental wild-type strain (WT) to find sTR for *afsS*, known as the mTR of ACT production (Lee et al. 2002). Through the following experiments, it was confirmed that the TRs selected as sTR for AfsS show a synergistic effect on ACT production when combined with AfsS. In addition, causal analysis of synergistic effects enabled us to further improve the synergistic effect of mTR and sTR and to propose new regulatory mechanisms.

Materials and methods

Bacterial strains and culture conditions

All the strains used in this experiment are listed in Table 1. *Escherichia coli* cells were cultured at 37 °C in Luria Bertani (LB) medium, supplemented with appropriate antibiotics when necessary. *E. coli* DH5 α was used for DNA amplification and manipulation, and *E. coli* JM110 was used for non-methylated DNA propagation for transformation into *S. coelicolor* A3(2) M145 was used as parental strain. R5⁻ complex media was used for cell growth and protoplast transformation (Kieser et al. 2000), and SMM, TSB, and R5MS media were used for antibiotic, i.e., ACT, production (Okamoto et al. 2009). For evaluation of secondary metabolites, spores were inoculated into a 250-ml baffled flask containing 50 ml of media with appropriate concentrations of antibiotic markers, and then shaken at 30 °C for 8 days. Samples (1 ml) were taken at various time points for ACT quantification and measurement of dry cell weight. pIBR25 was used as a cloning vector.

Microarray data analysis

Time-series microarray data were obtained from Gene Expression Omnibus (GEO) datasets (Barrett et al. 2007; Edgar et al. 2002). The GEO accession numbers of wild-type M145 and its *afsS* deletion mutant were GSE8084, GSE8086, and GSE8107 and GSE8110 and GSE8160, respectively (Lian et al. 2008). The raw intensities at every time point in each dataset were transformed to log₂ scales and normalized using the quantile normalization method (Bolstad et al. 2003). For the normalized dataset, log₂ values at specified time points were computed by subtracting the intensity of the initial time point from those of the sample time points to generate a fold-change matrix. The same process was done separately for all the five datasets, resulting in five fold-change matrices. To make the distribution of the five matrices identical, the five matrices were concatenated to create a new matrix, which was then normalized again using the quantile normalization method (Bolstad et al. 2003).

Table 1 Strains and plasmids used in this study

Strain, plasmid	Relevant information	Source or reference
Bacterial strains		
<i>E. coli</i>		
DH5 α	F- <i>endA1 glnV44 thi-1 recA1 relA1 gyrA96 deoR nupG Φ80dlacZΔM15 Δ(lacZYA-argF) U169, <i>hsdR17</i>(rK- mK+), λ</i>	Laboratory stock
JM110	<i>rpsL thr leu thi lacY galK galT ara tonA tsx dam dcm glnV44 Δ(lac-proAB) e14- [F' <i>traD36 proAB⁺ lac^f lacZΔM15] <i>hsdR17</i>(rK⁻mK⁺)</i></i>	Laboratory stock
<i>S. coelicolor</i> A3(2)		
M145	SCP1 ⁻ , SCP2 ⁻ , Pgl ⁺	Kieser et al. (2000)
Δ <i>rpfA</i>	SCO4677 deleted mutant	This study
Δ <i>phoU</i>	SCO4228 deleted mutant	This study
BG25	M145 harboring pIBR25	This study
BGPhoU	M145 containing pIBR25:: <i>sco4228</i>	This study
BGAfsS	M145 containing pAfsS25	This study
BG4677	SCO4677 deleted mutant containing pIBR25	This study
BG4228	SCO4228 deleted mutant containing pIBR25	This study
BG4677AfsS	SCO4677 deleted mutant containing pAfsS25	This study
BG4228AfsS	SCO4228 deleted mutant containing pAfsS25	This study
BG4677AfsSIA	SCO4677 deleted mutant containing pAfsSIA25	This study
BGCActAB	M145 harboring pCActAB25	This study
BGIActAB	M145 harboring pIActAB25	This study
BGIActC	M145 harboring pIActC25	This study
BGIActABC	M145 harboring pIActABC25	This study
BGIActCAB	M145 harboring pIActCAB25	This study
Plasmids		
pIBR25	pWHM3 carrying ermE* promoter (EcoRI/KpnI) from <i>Saccharopolyspora erythraea</i>	Thuy et al. (2005)
pIJ773	<i>aac(3)IV</i> (Apra ^R) + <i>oriT</i>	Gust et al. (2003)
Supercos1	<i>neo, bla</i>	Agilent
pAfsS25	pIBR25 based recombinant plasmid for expression of <i>afsS</i>	This study
pPhoU25	pIBR25-based recombinant plasmid for expression of <i>phoU</i>	This study
pCActAB25	pIBR25-based recombinant plasmid for constitutive expression of <i>actAB</i>	This study
pIActAB25	pIBR25-based recombinant plasmid for inducible expression of <i>actAB</i>	This study
pIActC25	pIBR25-based recombinant plasmid for inducible expression of <i>actC</i>	This study
pAfsSCA25	pIBR25-based recombinant plasmid for expression of <i>afsS</i> and constitutive expression <i>actAB</i>	This study
pAfsSIA25	pIBR25-based recombinant plasmid for expression of <i>afsS</i> and inducible expression <i>actAB</i>	This study
pIActABC25	pIBR25-based recombinant plasmid for inducible expression of <i>actAB</i> and <i>actC</i>	This study
pIActCAB25	pIBR25-based recombinant plasmid for inducible expression of <i>actC</i> and <i>actAB</i>	This study

The values of the five matrices were substituted by the values obtained from the above quantile normalization. Finally, the normalized matrices were smoothed using moving average method (window size = 3).

To identify the differentially expressed genes (DEGs) of the wild-type strain during growth phase changes, a modified time-series transcriptome analysis method (Hwang et al. 2005) was used as follows: in a matrix for the wild-type strain, (i) forward- and backward-smoothed fold-change profiles for each gene were numerically integrated over the time course to obtain the area under the smoothed fold-change profiles; (ii) reference fold-change profiles were generated through the

permutation-based random sampling from the smoothed fold-change matrix; (iii) a null distribution was empirically generated using the trapezoidal method for the areas of reference fold-change profiles; (iv) *P* values for each gene were calculated using the null distribution by one-tailed test; (v) three *P* values for each gene in the three datasets of the wild-type strain were combined using Stouffer's method; (vi) the genes showing significantly altered values of expression in all the three wild-type datasets were identified with a combined *P* value < 0.01. The DEGs identified from the above procedure are likely to be related to the genes for secondary metabolism in the wild-type cell.

For the clustering analysis of the gene expression profiles, the normalized time-series fold-change values of identified DEGs in the M145 and those of the same ID genes in *afsS* deletion mutant were collected, and a new DEG matrix with time-series fold-change values was generated. To find sTR genes for AfsS, i.e., mTR, the genes with similar profiles between the M145 and the *afsS* deletion mutant were identified from the newly generated DEG matrix through hierarchical clustering using the Pearson correlation.

RNA-seq data processing

We used time-series RNA-seq data of *S. coelicolor* A3(2) M145 obtained from GSE69350 (Jeong et al. 2016) for the screening of inducible promoters. This dataset was generated at four sampling time points depending on the growth phase, and the dataset was generated in duplicate at each time point (EE early exponential, ME mid exponential, LE late exponential, S stationary phase). The raw data of RNA-seq were normalized using spike-in controls in R, to compare the absolute expression values among the time-series data (Bar-Joseph et al. 2012). In this method, we used eight housekeeping genes as spike control (Li et al. 2015). After data processing, the global transcript profiles were clustered based on Pearson correlation coefficient to evaluate the similarity of the gene expression pattern along the growth phases (D’Haeseleer 2005). The hierarchical clustering was performed with “hclust” function in R using the Pearson method.

Measurement of undecylprodigiosin (RED) and actinorhodin (ACT)

The amounts of RED and ACT were measured at 530 and 640 nm, respectively, using a Multiskan Spectrum plate reader (Thermo Fisher Scientific, USA) following standard procedures (Kieser et al. 2000). For dry cell weight determinations, 2 mL of sampled cell broth (in triplicate) was collected in pre-weighted Eppendorf tube and dried at 70 °C for 4 days.

qPCR

The qPCR was performed with TOPreal SYBR Green PCR Kit (Enzynomics) on the Roche LightCycler® 480 real-time platform to quantify the absolute expression of specific mRNAs. Gene expression was normalized relative to *hrdB* (SCO5820) (Nieselt et al. 2010). All reactions were performed in technical triplicates. The *hrdB* was amplified from strain M145 using primers *hrdB_f* and *hrdB_r*, and the *actAB* was amplified from strain M145 using primers *actAB_f* and *actAB_r*. Table S1 shows the primers used for these experiments.

Results

Identification of sTR candidates for AfsS

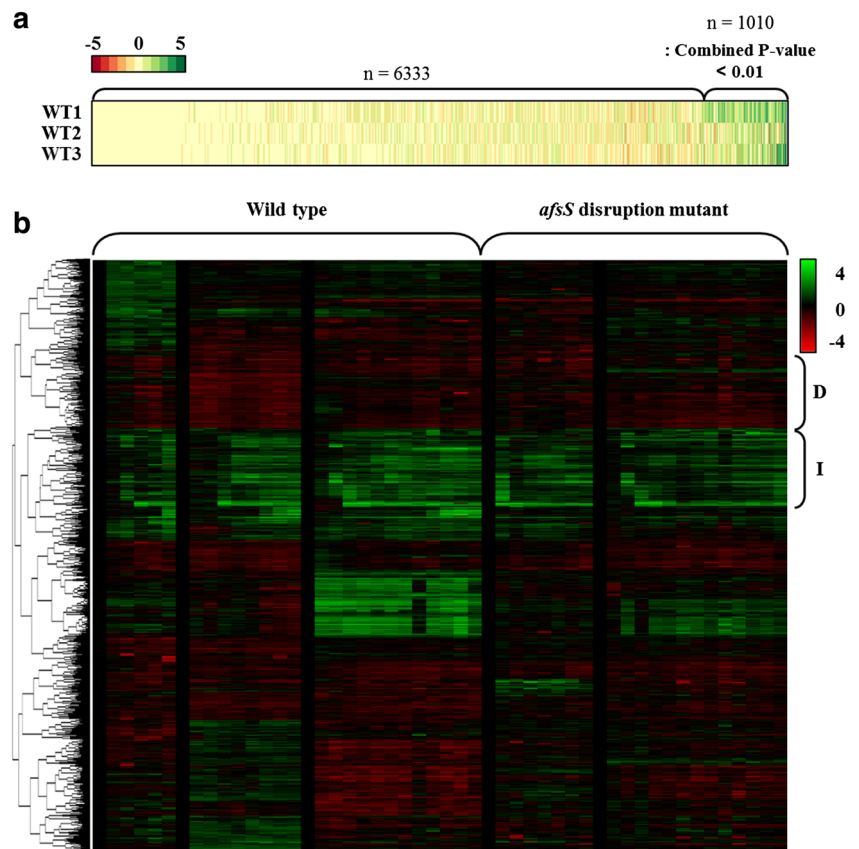
The procedure of clustering analysis is elaborated in the “Microarray data analysis” subsection in the “Materials and methods” section. To identify sTRs for AfsS, we first selected differentially expressed genes (DEGs) from the three datasets of wild-type M145 to catalog all the genes related to the secondary metabolism (Fig. 1a). As a result, 1010 genes among 7343 genes were selected as DEGs. Subsequently, clustering analysis between the M145 and *afsS* deletion mutant (M145(Δ *afsS*)) was performed to select genes showing the same profile in both strains among the DEGs (Fig. 1b). The basic premise of this analysis was that the genes classified into the same cluster in the M145 and the mutants would be related to the secondary metabolism but would not be affected by AfsS. We chose a cluster showing an increasing pattern during the stationary phase to screen the TRs related to ACT biosynthesis. The increasing cluster consisted of 109 genes, where 11 TRs were found and assigned as sTR candidates for AfsS (Table 2).

The objective of this experiment is to find sTRs for AfsS, which have a synergistic effect on the biosynthesis of ACT. Therefore, among the 11 sTR candidates, five TRs (SCO0608 (SlbR), SCO3579 (WblA), SCO4677 (RsfA), SCO7252 (NsdB), and SCO4228 (PhoU)) appearing to be related to ACT biosynthesis were selected. According to the literature survey, four of five candidates of sTR, excluding PhoU, were reported as repressor of ACT production (Hindra et al. 2014; Lee et al. 2013; Yang et al. 2012; Zhang et al. 2007). Among them, when the repression is removed by gene deletion, the sTR with the largest increase in ACT production was RsfA. Therefore, RsfA was finally selected as sTR because it was expected to maximize the synergistic effect on ACT production along with the overexpression of AfsS. In the case of PhoU, the impact on the production of ACT has not been reported. However, it is strongly anticipated that it is related to the PhoR-PhoP system that affects the production of ACT. The main advantage of clustering analysis is that it can find sTRs without knowing the TR network. If the double mutant (The strain that combines the effects of mTR and sTR is hereinafter referred to as “double mutant”), PhoU deletion and AfsS overexpression, shows a synergistic effect, the robustness of the clustering analysis could be confirmed. Therefore, PhoU and RsfA were finally selected as potential sTRs and subjected to experiments to demonstrate and confirm their synergistic effects on ACT production by the combination with AfsS.

Confirmation of the synergistic effect of PhoU on AfsS

PhoU has been considered as a TR associated with a two-component PhoR-PhoP system, but the exact function of PhoU in *S. coelicolor* remains unclear (Santos-Beneit et al.

Fig. 1 Transcriptome analysis for wild-type and *afsS* disruption mutant. **a** Identification of differentially expressed genes (DEGs) from three datasets of wild-type *S. coelicolor* A3(2) M145 (combined *p* value < 0.01). 1010 genes were selected as DEGs. **b** Clustering analysis to find genes with similar transcriptome profile for wild-type M145 and *afsS* deletion mutant among the DEGs. D decrease profile, I increase profile



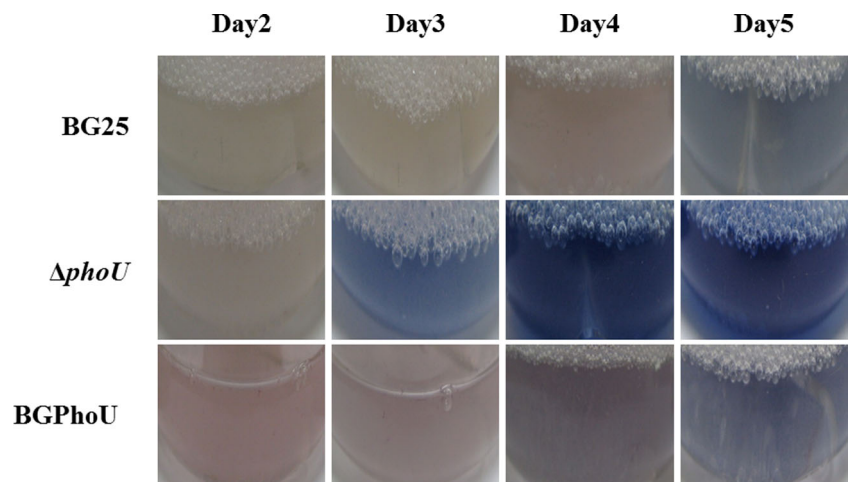
2009). To investigate the role of PhoU in ACT biosynthesis, a *phoU*-amplified mutant (BGPhoU) and a *phoU* deletion mutant (M145 $\Delta phoU$) were constructed. Since the PhoR-PhoP system controls both primary and secondary metabolism in the phosphate limitation environment (Sola-Landa et al. 2003), ACT productions of BGPhoU, M145 $\Delta phoU$, and M145 were firstly measured on SMM solid agar plates with varying phosphate concentrations to approximately figure out what is the optimum concentration of phosphate for ACT

Table 2 List of independent regulators found through clustering analysis using M145 strain and *afsS* disruption mutant

SCO no.	Name	Function
SCO0608		Regulatory protein
SCO1699		Transcriptional regulator
SCO1839		Transcriptional regulator
SCO3217	<i>cdaR</i>	Transcriptional regulator
SCO3323	<i>bldN</i>	RNA polymerase sigma factor
SCO3579	<i>wblA</i>	Regulatory protein
SCO4228	<i>phoU</i>	Phosphate transport system regulator
SCO4677	<i>rsfA</i>	Antagonistic regulator of σ^F
SCO4768	<i>bldM</i>	Two-component regulator
SCO5877	<i>redD</i>	Transcriptional regulator
SCO7252		Regulatory protein

production (Fig. S1). As a result, SMM media without phosphate was selected for ACT production, and all strains were cultured in SMM liquid media without phosphate for 5 days. When the ACT yields of the two mutants were compared to that of BG25 (M145 harboring pIBR25), no significant differences were observed between BGPhoU (12.9 mg/L) and BG25 (11.8 mg/L), but the $\Delta phoU$ mutant showed an increased ACT yield (69.1 mg/L) (Fig. 2), suggesting that PhoU is a negative TR on ACT production under such conditions. After confirming the role of PhoU, the double-mutant BG4228AfsS ($\Delta phoU$ pIBR25::*afsS*) was constructed to confirm the synergistic effect of *phoU* deletion and *afsS* overexpression on the production of ACT. The ACT yield of the double mutant was then compared with that of the single mutants, BG4228 ($\Delta phoU$ pIBR25) and BGAfsS (M145 pIBR25::*afsS*). The double-mutant BG4228AfsS yielded the highest titer (151.4 mg/L), which was 9 times higher than that of BGAfsS (M145 pIBR25::*afsS*; 16.3 mg/L) and 63 times higher than that of BG4228 (2.37 mg/L) (Fig. 3a). Since AfsS is a pleiotropic TR for other antibiotics biosynthesis as well in *S. coelicolor*, RED production was also measured in the same strains shown above, and the trends were similar (Fig. S2 A). These results indicate that the effect of *afsS* overexpression and *phoU* deletion on ACT and RED production is mutual and additive.

Fig. 2 Characterization of the role of PhoU on ACT production. The effect of *phoU* disruption and overexpression on ACT production by comparing three strains (M145, $\Delta phoU$, and BGPhoU) for 5 days in SMM liquid media without phosphate



Confirmation of the synergistic effect of RsfA on AfsS

RsfA (SCO4677), previously known as anti-sigma factor F, exerts a negative effect on ACT production and cell morphological differentiation (Kim et al. 2008). When BG4677($\Delta rsfA$ pIBR25) and BGAfsS were grown in R5⁻ complex media, they showed 1.5- and 3.2-fold increases in ACT yield compared to that of BG25, respectively. Whereas the double mutant,

BG4677AfsS ($\Delta rsfA$ pIBR25::*afsS*), showed an 8-fold increase in ACT yield under the same condition, confirming that *afsS* overexpression and *rsfA* deletion have a synergistic effect on ACT production (Fig. 3c). In terms of RED production, BG4677AfsS displayed an 8-fold increase in RED titer compared to that of BG25, whereas both BG4677 and BGAfsS did not show any significant positive effects on RED production (Fig. S2 B). These results also indicate that the effect of *afsS*

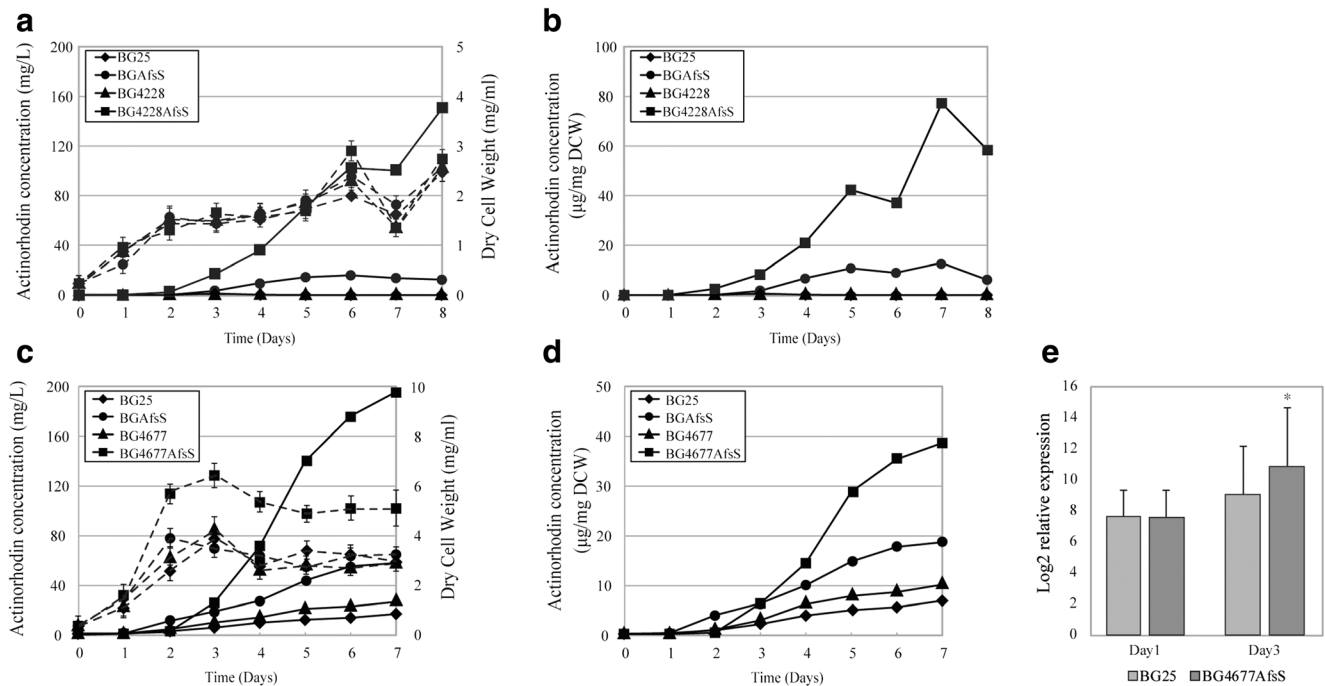


Fig. 3 ACT quantitation and cell growth comparison in double mutants. **a** The yield of ACT, cell growth, and **b** the specific yield of ACT in each strain. BGAfsS (M145 pIBR25::*afsS*), BG4228 ($\Delta phoU$ pIBR25), control (BG25), and BG4228AfsS ($\Delta phoU$ pIBR25::*afsS*) cultured in liquid SMM media without phosphate. Even though the effects of BGAfsS and BG4228 on ACT were not significant, the effects of BG4228AfsS on ACT was significant. The solid lines indicate the ACT concentration, and the dashed lines indicate the dry cell weight. **c** The yield of ACT, cell growth, and **d** the specific yield of ACT in each strain.

BGAfsS (M145 pIBR25::*afsS*), BG4677 ($\Delta rsfA$ pIBR25), control (BG25), and BG4677AfsS ($\Delta rsfA$ pIBR25::*afsS*) cultured in liquid R5⁻ complex media. The yield of ACT of BGAfsS and BG4677 was increased by 1.5- and 3.2-fold, respectively, compared with that of BG25. The ACT yield of BG4677AfsS increased by 8-fold compared to that of BG25. The specific yield of BG4677AfsS increased by 4.8-fold compared to that of BG25. The solid lines indicate the ACT concentration, and the dashed lines indicate the dry cell weight. **e** Relative mRNA expression of *actAB* in BG25 and BG4677AfsS at days 1 and 3, respectively. * $P \leq 0.05$

overexpression and *rsfA* deletion on ACT and RED production is mutual. The above results could validate our clustering analysis to find sTRs for the target mTR, AfsS.

The 8-fold increase in ACT yield of BG4677AfsS compared to that of BG25 was resulted from the combination of 1.6-fold increase in cell mass and 4.8-fold increase in its specific yield (Fig. 3c, d). It was somewhat expected that inhibition of cell growth might occur in the case of BG4677AfsS owing to the ACT secretion and/or toxicity of ACT itself. Surprisingly, however, an opposite result was acquired. BG4677AfsS showed ca. 60% increase in cell growth compared to that of BG25 despite higher ACT production (Fig. 3c). One possible explanation would be that *actAB* induction by ACT or its three-ring intermediate (S)-DNPA synthesis, which may confer additional resistance to the cell by ACT overproduction, resulting in cell growth enhancement (Xu et al. 2012). When comparing the expression of *actAB* in BG25 and BG4677AfsS, it was confirmed that the expression level of *actAB* in BG4677AfsS increased about 3.5 times than that of BG25. (Fig. 3e). This result agrees well with our assumption that the additional overexpression of *actAB* can further improve the ACT yield of BG4677AfsS.

Inducible overexpression of *actAB* increases not only ACT production but also final cell mass

In order to prove whether the increase in cell mass of BG4677AfsS by overexpression of *actAB* can increase ACT yield, *actAB* was overexpressed in the M145. To construct the strain overexpressing *actAB*, transformation of pCActAB25 having a constitutive strong *ermE* promoter into BG25 was performed (Table 1). However, the BGCActAB (BG25 pIBR25::*actAB*) strain showed very sluggish cell growth in R5⁻ media. On R5⁻ agar plate, BG25 colonies appeared within 2 days, whereas the colonies of BGCActAB appeared after 7 days. In R5⁻ liquid medium, the BG25 strain followed a normal growth curve, but the growth of BGCActAB did not start for 4 days (Fig. S3). Surprisingly, the cell growth of BGCActAB starts to recover after 5 days and the mutant outgrew BG25 by 150% after 7 days (Fig. S3) and its ACT yield was 4-fold higher than that of BG25 at 7 days (data was not shown). These results clearly demonstrated that overexpression of *actAB*, the putative efflux pumps of ACT, has a positive effect on final cell mass and ACT production but does prolong the lag phase. We hypothesized that excessive *actAB* expression in earlier cell growth stage might be the cause of initial sluggish cell growth, and the possible solution to overcome this would be expression of *actAB* using inducible promoter at late exponential phase.

Promoter used for overexpression of efflux pumps requires high expression level of target protein starting from late exponential phase. To discover such additional inducible promoters, another clustering analysis was performed using our

own experimental RNA-seq data taken at four different time points. The raw data of RNA-seq were processed with spike-in normalization and clustered based on Pearson correlation coefficient. All the genes were grouped into 12 clusters (Fig. 4). In particular, we could confirm that the ACT cluster including the putative efflux pumps belong to cluster 7. The genes in cluster 7 were listed according to the fold changes in the ratio of the corresponding gene expression level of the stationary phase to that of the early exponential phase (i.e.,

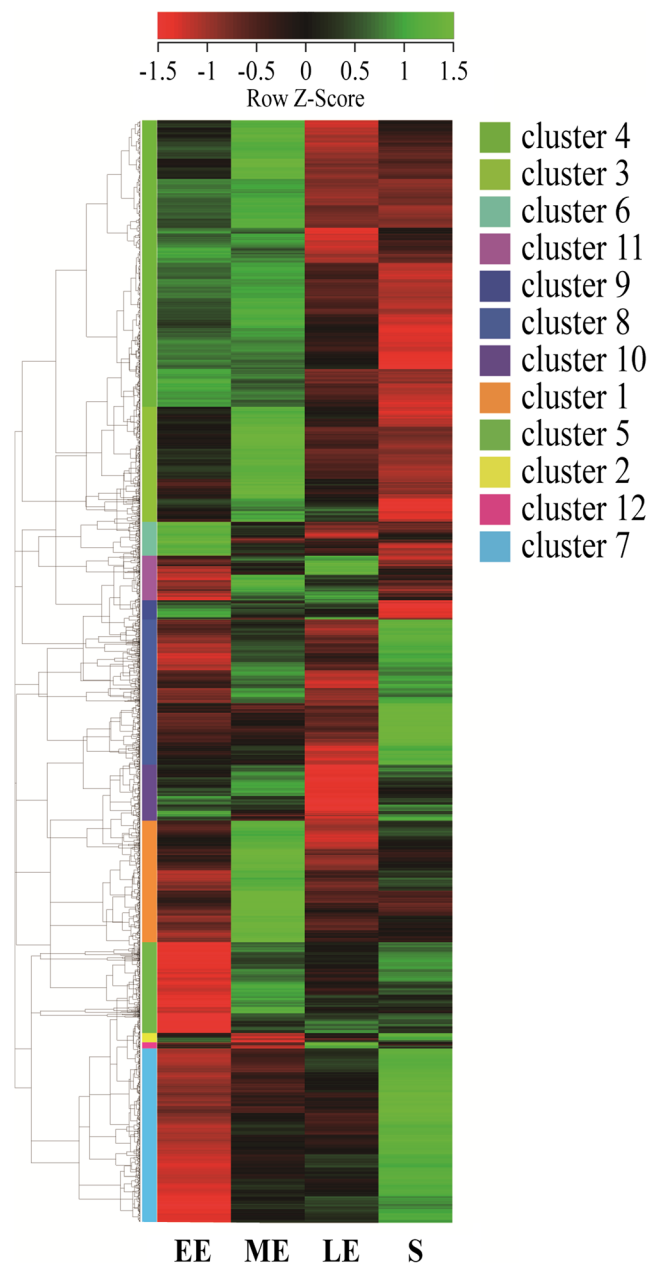


Fig. 4 Time-series gene expression data analysis. A heat map and hierarchical clusters of gene expression across growth phase. The expression profiles of all the genes were analyzed by using Pearson correlation. This identified 12 major groups. EE early exponential, ME mid exponential, LE late exponential, S stationary)

S/EE), to discover any promoters with the desired expression profile. Among the selected candidates, the promoter of SCO4677 was chosen as the inducible promoter to express the efflux pump since its function is well characterized and its fold-change ratio (S/EE) was very high (Table 3). pIActAB25 was constructed for inducible expression of efflux pump (ActA-ActB) and transformed into *S. coelicolor* M145 strain by protoplast fusion to yield BGIActAB. In the case of BGIActAB grown in R5⁻ liquid media containing 10 µg/ml thioestrepton for 5 days, its dry cell weight and specific yield of ACT increased 2- and 2.1-fold, respectively, compared to those of BG25 (Fig. 5a, b). BGIActAB exhibited an c.a. 4-fold increase in ACT yield, compared to that of BG25 (Fig. 5c). This result demonstrates that the optimal overexpression

of *actAB* under the control of the screened inducible promoter is able to increase not only ACT production but also the final cell mass.

Inducible overexpression of *actAB* for high ACT producers with the combination of sTR and *afsS*

Since the cell mass of BGIActAB achieved in R5⁻ liquid media was higher than that of BG4677AfsS, we reasoned that the additional overexpression of *actAB* in the background of BG4677AfsS would give an improved production of ACT. First, pAfsSIA25, in which *actAB* and *afsS* genes were inserted in opposite directions, was constructed to avoid interference of the two gene expressions. Then, the plasmid was

Table 3 List of cluster 7

SCO no.	Name	Function	RNA expression level				Ratio (S/EE)
			EE	ME	LE	S	
SCO4175		Hypothetical protein	4	202	1291	27,799	6388
SCO4174		Hypothetical protein	7	116	679	16,078	2314
SCO0930		Lipoprotein	9	33	180	15,217	1783
SCO3288		Hypothetical protein	4	13	393	5531	1522
SCO2519		Hypothetical protein	41	237	40,442	60,427	1481
SCO1630	<i>rarA</i>	Hypothetical protein	19	103	6448	19,430	1000
SCO1161		Hypothetical protein	5	11	189	4219	905
SCO1160		Hypothetical protein	11	20	509	9596	838
SCO4677	<i>rsfA</i>	Regulatory protein	21	238	6307	17,207	828
SCO1628	<i>rarC</i>	Hypothetical protein	9	48	2624	7138	814
SCO0752	<i>salO</i>	protease	3	8	30	2131	749
SCO1627	<i>rarD</i>	ATP-GTP binding protein	11	59	2899	7756	677
SCO6795		Hypothetical protein	4	40	1422	2868	648
SCO1629	<i>rarB</i>	Hypothetical protein	13	47	2893	8099	641
SCO3289		Large membrane protein	18	39	705	11,022	615
SCO1159		Hypothetical protein	3	4	100	1777	592
SCO4947	<i>narG3</i>	Nitrate reductase Subunit alpha NarG3	45	38	647	26,086	582
SCO2218		Lipoprotein	2	3	22	983	517
SCO3290		Hypothetical protein	12	31	414	6061	504
SCO1860		Hypothetical protein	65	434	25,542	30,938	473
SCO6682	<i>ramS</i>	Hypothetical protein	29	145	1279	13,569	469
SCO0644		Hypothetical protein	32	76	283	14,165	449
SCO0382		UDP-glucose/GDP-mannose Dehydrogenase	14	145	1203	5975	420
SCO6796		Hypothetical protein	6	35	1243	2676	413
SCO1626	<i>rarE</i>	Cytochrome P450	62	227	11,186	25,152	404
SCO4948	<i>narH3</i>	Nitrate reductase subunit beta NarH3	17	21	131	6748	395
SCO0685		Hypothetical protein	12	132	1987	4773	382
SCO5895	<i>redI</i>	Methyltransferase	21	488	4180	7939	379
SCO6798		Hypothetical protein	7	41	1453	2698	376
SCO0393		Transferase	11	64	603	4025	374

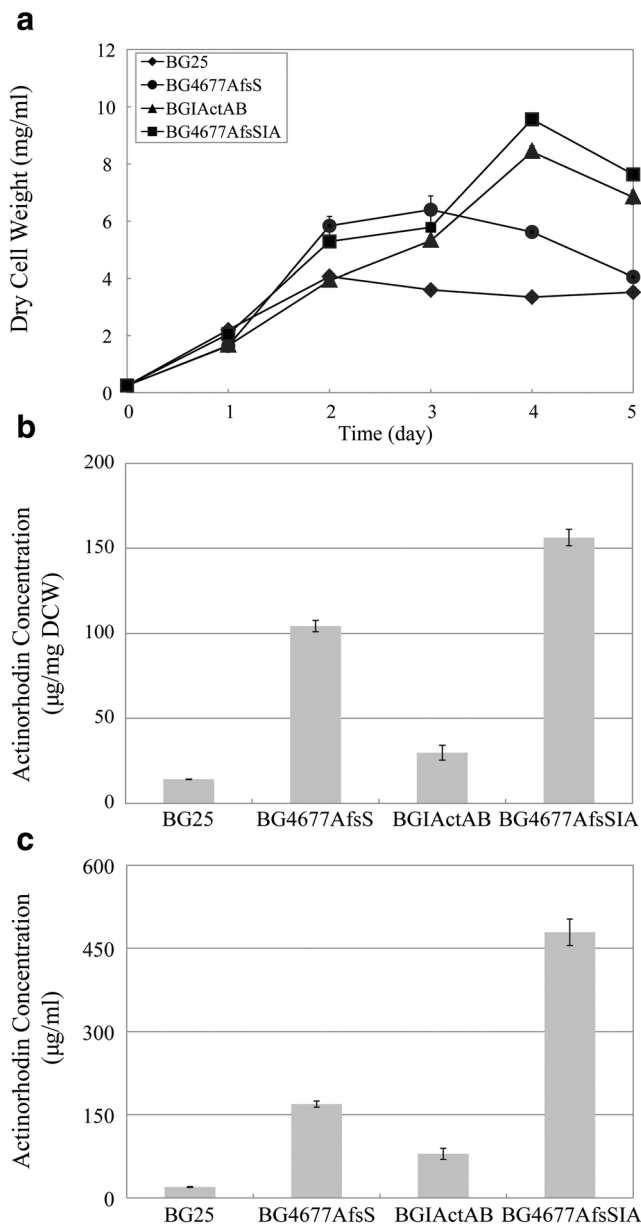


Fig. 5 Effects of double-mutant and inducible overexpression of efflux pump on cell growth and ACT production. **a** Growth of BGIActAB and BG4677AfsSIA, which both overexpress the efflux pump ActA-ActB inducibly, was increased by 2-fold compared to that of BG25 (M145 harboring pIBR25). **b** The specific yield of BGIActAB was increased by 2-fold compared to that of BG25, and BG4677AfsSIA was increased by 1.5-fold compared to that of BG4677AfsS. **c** The ACT yield of BGIActAB was increased by 4-fold compared to that of BG25, and BG4677AfsSIA was increased by 3-fold compared to that of BG4677AfsS and increased by 24-fold compared to that of BG25. (ACT measurement was done at day 5)

introduced into the BG4677 strain by protoplast transformation to yield BG4677AfsSIA. After 4-day growth of BG4677AfsSIA, its cell mass and ACT yield were 9.57 mg/ml of DCW and 480 mg/L, respectively. The final cell mass was more than two times higher than that of its parental strain BG25 (Fig. 5a–c), and ACT titer was the highest ever reported.

Discussion

Identification of sTRs while the overexpression of strong mTR is present is a formidable task and very important for industrial mass production of antibiotics, since secondary metabolism is often simultaneously regulated by various TRs. However, due to the complexity of the TR network, it is difficult to find such sTRs for any specific mTR (Lv et al. 2014). In this study, we applied a clustering analysis to discover such sTRs by comparing time-series transcriptome data of wild-type and specified mTR deletion mutant (here, *afsS*) without the need to understand the regulatory network of corresponding antibiotic biosynthesis (here, ACT).

The major advantage of clustering analysis is its accurate screening capability of sTRs for a specified target mTR. In the case of ACT, PhoU (SCO4228) is a good example. Despite the uncertainty of the function and regulatory network of PhoU, PhoU was identified as a sTR for AfsS (SCO 4425). Although each of the effect of *phoU* deletion and *afsS* overexpression on ACT production was negligible, a significant increase in the production of ACT was observed in the double mutant, BG4228AfsS. This result did not appear to be caused by a simple additive effect but by a synergistic effect via unknown interactions. We reasoned that PhoU and AfsS might influence each other within its TR network, resulting in a higher production of ACT. In *S. coelicolor*, the transcription of *afsS* is repressed by the phosphorylated form of PhoP, whose phosphorylation is controlled by PhoR (Santos-Beneit et al. 2009). Thus, the biosynthesis of ACT is very likely to be repressed in the presence of phosphorylated PhoP, despite the overexpression of *afsS*. Especially, it has been reported that the kinase activity of PhoR is controlled by PhoU in *Escherichia coli* (Gardner et al. 2014) and *Aquifex aeolicus* (Oganesyan et al. 2005). Therefore, it is possible to assume that the PhoU in *S. coelicolor* can control the PhoR-PhoP system and may affect the transcription of *afsS*. In fact, a synergistic effect on ACT yield was observed in BG4228AfsS strain, which can be strongly anticipated as a result of relieving AfsS repression by blocking PhoP phosphorylation through *phoU* deletion. This is consistent with the assumption that PhoU of *S. coelicolor* controls the PhoR-PhoP system. Furthermore, it suggests that PhoU, a selected sTR for AfsS, is an upper layer TR of AfsS that regulates the negative interaction of AfsS and PhoP by controlling phosphorylation of PhoP.

In the case of the double mutant, BG4677AfsS, the specific yield of ACT was increased by 4.8-fold compared to that of BG25. The specific yield of BG4677 and BGAfsS showed 1.5- and 3.2-fold increase compared to that of BG25, respectively. This result can be interpreted as the increase in yield of ACT in BG4677AfsS is due to the simple addition of *rsfA* deletion and *afsS* overexpression effect on ACT production. Therefore, it is reasonable to conclude that RsfA and AfsS independently affect ACT

production in the TR network. This result demonstrates that the selected sTR for the mTR through the clustering analysis actually functions independently.

Furthermore, a synergistic effect was observed in terms of ACT yield of BG4677AfsS, mainly due to an increase in cell mass. To our surprise, the increase in cell mass was hypothesized to be somewhat related to the increased expression of the *actAB* induced by the increased amount of ACT in the cell (Xu et al. 2012). We attempted to demonstrate the effect of efflux pump overexpression on increase in cell mass via overexpression of *actAB*. The overexpression level and expression timing of *actAB* appeared to greatly affect cell growth. When they were overexpressed in early growth phase, very long lag time was observed in the cell growth, whereas, when they were overexpressed in a late exponential phase, increase in cell growth was observed. The BGIActAB which overexpresses the *actAB* using an inducible promoter (promoter of SCO4677) in the M145 greatly increased not only the cell mass but also the specific yield of ACT. Since the cell mass of the BGIActAB was even higher than that of BG4677AfsS, fine control of the efflux pump overexpression in BG4677AfsS mutant strain was expected to result further increase in the productivity of ACT, which was confirmed through our study.

In addition, since the efflux pump, in general, has the function of pumping out toxic substances (Poole 2007), it was expected that the strain which overexpresses the efflux pump (ActA-ActB) show higher secretion of ACT. Unlike our prediction, higher ACT secretion was not observed in our experiment, and the specific secretion ability of the BGIActAB was reduced by 2.8-fold compared to that of parental strain BG25 (Fig. S4 A). Instead, the strain which overexpresses the *actC* (one of the three putative efflux pumps of ACT biosynthesis cluster) using an inducible promoter used in the aforementioned experiment (BGIActC) showed that the specific secretion ability of the cell increased 2.2-fold compared to that of the parental strain BG25 (Fig. S4 A). These results suggest that ActC functions as an actual efflux pump of ACT, and ActA-ActB has other functions that enhance ACT resistance. This is consistent with the two-step model for ACT export and resistance, in which ActA-ActB is required for efficient production of ACT and increases resistance to ACT (Xu et al. 2012).

In summary, we could find sTRs of mTR (e.g., AfsS) for overproduction of desired antibiotics through clustering analysis using transcriptome data of the wild-type strain and the mTR deletion mutant without prior understanding of complex regulatory network of TR. Even though the synergistic effects of all five sTRs on mTR have not been tested, it was well demonstrated that the clustering analysis is suitable for selecting sTR candidates for mTR. Analysis of the synergistic effects of the sTR candidates allowed us to suggest an unknown regulatory mechanism among the TRs and predict which to optimize in order to further increase the production of ACT. The ACT yield of the final strain, BG4677AfsSIA, is

the highest ever reported, and this study is the first successful report of antibiotic overproduction by the combination of two TRs (here, sTR and mTR). These strategies can be applied to increase the production of any secondary metabolites in Actinobacteria.

Acknowledgments This research was supported by the National Research Foundation of Korea(NRF) funded by the Ministry of Science, ICT and Future Planning (2016953757), and by Korea Institute of Planning and Evaluation for Technology in Food, Agriculture, Forestry and Fisheries (IPET) through Agri-Bio industry Technology Development Program, funded by Ministry of Agriculture, Food and Rural Affairs (MAFRA)(116139-03-1-SB010), and by the Institute for Basic Science (IBS-R13-G1).

Compliance with ethical standards

Conflict of interest The authors declare that they have no conflict of interest.

Ethical approval This article does not contain any studies with human participants or animals performed by any of the authors.

References

- Baltz RH (2008) Renaissance in antibacterial discovery from *actinomycetes*. *Curr Opin Pharmacol* 8(5):557–563. <https://doi.org/10.1016/j.coph.2008.04.008>
- Bar-Joseph Z, Gitter A, Simon I (2012) Studying and modelling dynamic biological processes using time-series gene expression data. *Nat Rev Genet* 13(8):552–564. <https://doi.org/10.1038/nrg3244>
- Barrett T, Troup DB, Wilhite SE, Ledoux P, Rudnev D, Evangelista C, Kim IF, Soboleva A, Tomashevsky M, Edgar R (2007) NCBI GEO: mining tens of millions of expression profiles—database and tools update. *Nucleic Acids Res* 35(Database issue):D760–D765. <https://doi.org/10.1093/nar/gk1887>
- Bolstad BM, Irizarry RA, Astrand M, Speed TP (2003) A comparison of normalization methods for high density oligonucleotide array data based on variance and bias. *Bioinformatics* 19(2):185–193
- D’Haeseleer P (2005) How does gene expression clustering work? *Nat Biotechnol* 23(12):1499–1501. <https://doi.org/10.1038/nbt1205-1499>
- Edgar R, Domrachev M, Lash AE (2002) Gene expression omnibus: NCBI gene expression and hybridization array data repository. *Nucleic Acids Res* 30(1):207–210
- Eisen MB, Spellman PT, Brown PO, Botstein D (1998) Cluster analysis and display of genome-wide expression patterns. *Proc Natl Acad Sci* 95(25):14863–14868
- Gardner SG, Johns KD, Tanner R, McCleary WR (2014) The PhoU protein from *Escherichia coli* interacts with PhoR, PstB, and metals to form a phosphate-signaling complex at the membrane. *J Bacteriol* 196(9):1741–1752. <https://doi.org/10.1128/jb.00029-14>
- Gust B, Challis GL, Fowler K, Kieser T, Chater KF (2003) PCR-targeted *Streptomyces* gene replacement identifies a protein domain needed for biosynthesis of the sesquiterpene soil odor geosmin. *Proc Natl Acad Sci U S A* 100(4):1541–1546. <https://doi.org/10.1073/pnas.0337542100>
- Hindra MMJ, Jones SE, Elliot MA (2014) Complex intra-operonic dynamics mediated by a small RNA in *Streptomyces coelicolor*. *PLoS One* 9(1):e85856. <https://doi.org/10.1371/journal.pone.0085856>

- Hwang D, Rust AG, Ramsey S, Smith JJ, Leslie DM, Weston AD, de Atauri P, Aitchison JD, Hood L, Siegel AF, Bolouri H (2005) A data integration methodology for systems biology. *Proc Natl Acad Sci U S A* 102(48):17296–17301. <https://doi.org/10.1073/pnas.0508647102>
- Jeong Y, Kim JN, Kim MW, Bucca G (2016) The dynamic transcriptional and translational landscape of the model antibiotic producer *Streptomyces coelicolor* A3(2). *Nat Commun* 7:11605. <https://doi.org/10.1038/ncomms11605>
- Kieser T, Bibb MJ, Buttner MJ, Chater KF, Hopwood DA (2000) Practical *streptomyces* genetics. The John Innes Foundation, Norwich
- Kim ES, Song JY, Kim DW, Chater KF, Lee KJ (2008) A possible extended family of regulators of sigma factor activity in *Streptomyces coelicolor*. *J Bacteriol* 190(22):7559–7566. <https://doi.org/10.1128/jb.00470-08>
- Lee PC, Umeyama T, Horinouchi S (2002) *afsS* is a target of AfsR, a transcriptional factor with ATPase activity that globally controls secondary metabolism in *Streptomyces coelicolor* A3(2). *Mol Microbiol* 43(6):1413–1430
- Lee HN, Kim JS, Kim P, Lee HS, Kim ES (2013) Repression of antibiotic downregulator WblA by AdpA in *Streptomyces coelicolor*. *Appl Environ Microbiol* 79(13):4159–4163. <https://doi.org/10.1128/aem.00546-13>
- Li S, Wang J, Li X, Yin S, Wang W, Yang K (2015) Genome-wide identification and evaluation of constitutive promoters in *streptomyces*. *Microb Cell Factories* 14(1):172. <https://doi.org/10.1186/s12934-015-0351-0>
- Lian W, Jayapal KP, Charaniya S, Mehra S, Glod F, Kyung YS, Sherman DH, Hu WS (2008) Genome-wide transcriptome analysis reveals that a pleiotropic antibiotic regulator, AfsS, modulates nutritional stress response in *Streptomyces coelicolor* A3(2). *BMC Genomics* 9:56. <https://doi.org/10.1186/1471-2164-9-56>
- Lv Q, Cheng R, Shi T (2014) Regulatory network rewiring for secondary metabolism in *Arabidopsis thaliana* under various conditions. *BMC Plant Biol* 14:180. <https://doi.org/10.1186/1471-2229-14-180>
- Nieselt K, Battke F, Herbig A, Bruheim P, Wentzel A, Jakobsen ØM, Sletta H, Alam MT, Merlo ME, Moore J, Omara WAM, Morrissey ER, Juarez-Hermosillo MA, Rodríguez-García A, Nentwich M, Thomas L, Iqbal M, Legaie R, Gaze WH, Challis GL, Jansen RC, Dijkhuizen L, Rand DA, Wild DL, Bonin M, Reuther J, Wohlleben W, Smith MCM, Burroughs NJ, Martín JF, Hodgson DA, Takano E, Breitling R, Ellingsen TE, Wellington EMH (2010) The dynamic architecture of the metabolic switch in *Streptomyces coelicolor*. *BMC Genomics* 11:10–10. <https://doi.org/10.1186/1471-2164-11-10>
- Oganesyan V, Oganesyan N, Adams PD, Jancarik J, Yokota HA, Kim R, Kim S-H (2005) Crystal structure of the “PhoU-like” phosphate uptake regulator from *Aquifex aeolicus*. *J Bacteriol* 187(12):4238–4244
- Ohnishi Y, Yamazaki H, Kato J-Y, Tomono A, Horinouchi S (2005) AdpA, a central transcriptional regulator in the A-factor regulatory cascade that leads to morphological development and secondary metabolism in *Streptomyces griseus*. *Biosci Biotechnol Biochem* 69(3):431–439. <https://doi.org/10.1271/bbb.69.431>
- Okamoto S, Taguchi T, Ochi K, Ichinose K (2009) Biosynthesis of actinorhodin and related antibiotics: discovery of alternative routes for quinone formation encoded in the act gene cluster. *Chem Biol* 16(2):226–236. <https://doi.org/10.1016/j.chembiol.2009.01.015>
- Park SS, Yang YH, Song E, Kim EJ, Kim WS, Sohng JK, Lee HC, Liou KK, Kim BG (2009) Mass spectrometric screening of transcriptional regulators involved in antibiotic biosynthesis in *Streptomyces coelicolor* A3(2). *J Ind Microbiol Biotechnol* 36(8):1073–1083. <https://doi.org/10.1007/s10295-009-0591-2>
- Patra B, Schluttenhofer C, Wu Y, Pattanaik S, Yuan L (2013) Transcriptional regulation of secondary metabolite biosynthesis in plants. *Biochim Biophys Acta* 1829(11):1236–1247. <https://doi.org/10.1016/j.bbagr.2013.09.006>
- Poole K (2007) Efflux pumps as antimicrobial resistance mechanisms. *Ann Med* 39(3):162–176. <https://doi.org/10.1080/07853890701195262>
- Santos-Beneit F, Rodríguez-García A, Sola-Landa A, Martín JF (2009) Cross-talk between two global regulators in *Streptomyces*: PhoP and AfsR interact in the control of *afsS*, *pstS* and *phoRP* transcription. *Mol Microbiol* 72(1):53–68. <https://doi.org/10.1111/j.1365-2958.2009.06624.x>
- Sola-Landa A, Moura RS, Martín JF (2003) The two-component PhoR-PhoP system controls both primary metabolism and secondary metabolite biosynthesis in *Streptomyces lividans*. *Proc Natl Acad Sci U S A* 100(10):6133–6138. <https://doi.org/10.1073/pnas.0931429100>
- Thuy ML, Kharel MK, Lamichhane R, Lee HC, Suh JW, Liou K, Sohng JK (2005) Expression of 2-deoxy-scyllo-inosose synthase (*kanA*) from kanamycin gene cluster in *Streptomyces lividans*. *Biotechnol Lett* 27(7):465–470. <https://doi.org/10.1007/s10529-005-2222-y>
- Valouev A, Johnson DS, Sundquist A, Medina C, Anton E, Batzoglou S, Myers RM, Sidow A (2008) Genome-wide analysis of transcription factor binding sites based on ChIP-Seq data. *Nat Methods* 5(9):829–834. <https://doi.org/10.1038/nmeth.1246>
- Xu Y, Willems A, Au-Yeung C, Tahlan K, Nodwell JR (2012) A two-step mechanism for the activation of actinorhodin export and resistance in *Streptomyces coelicolor*. *MBio* 3(5):e00191–e00112. <https://doi.org/10.1128/mBio.00191-12>
- Yang Y-H, Song E, Kim J-N, Lee B-R, Kim E-J, Park S-H, Kim W-S, Park H-Y, Jeon J-M, Rajesh T, Kim Y-G, Kim B-G (2012) Characterization of a new ScbR-like γ -butyrolactone binding regulator (SlbR) in *Streptomyces coelicolor*. *Appl Microbiol Biotechnol* 96(1):113–121. <https://doi.org/10.1007/s00253-011-3803-4>
- Zhang L, Li WC, Zhao CH, Chater KF, Tao MF (2007) NsdB, a TPR-like-domain-containing protein negatively affecting production of antibiotics in *Streptomyces coelicolor* A3 (2). *Wei Sheng Wu Xue Bao* 47(5):849–854